1-mm wave ESR spectrometer

W. Bryan Lynch,[a] Keith A. Earle, and Jack H. Freed

Baker Laboratory of Chemistry, Cornell University, Ithaca, New York 14853

(Received 8 March 1988; accepted for publication 2 May 1988)

An ESR spectrometer operating at 250-GHz frequency (1.22-mm wavelength) and 9-T magnetic field is described. The utilization of far-infrared (FIR) technology greatly simplifies its design and performance. Good frequency and field stability are achieved by unique designs which also conveniently permit the magnetic field to be swept. The potential utility of FIR–ESR is illustrated with examples of spectra from polycrystalline and liquid samples. In the latter case the increased spectral sensitivity to motional dynamics is stressed. Several ways in which the FIR–ESR spectrometer may be improved are also discussed.

INTRODUCTION

In recent years we have seen a growth of interest in ESR spectroscopy performed at high fields using superconducting magnets and high frequencies. This is predated by analogous developments in NMR with the objectives of increasing sensitivity and increasing the resolution of complex spectra. Notable in the electron-spin-resonance (ESR) field has been the development and application of an ESR spectrometer working at $\lambda = 2$ mm (i.e., 148 GHz) corresponding to 5.3-T fields by Lebedev and co-workers.[1] They have reported on nitroxide spectra seen in the liquid and solid phases, and they emphasize the significant resolution improvement for determining g tensors and, more recently, for slow motional studies. Also, the sensitivity is significantly better than that of conventional ESR spectrometers. More recently Möbius has reported on an ESR spectrometer operating at 94 GHz ($\lambda = 3.2$ mm) with similar advantages.[2]

As one attempts to go to even higher fields and frequencies, it becomes increasingly difficult to utilize microwave technology, although this proved possible for $\lambda = 2$–3 mm. Waveguides and cavities become exceedingly small and lossy.

In this article we describe a new ESR spectrometer we have constructed to operate at $\lambda = 1.2$ mm corresponding to 250-GHz frequency and 9-T fields.[3a] We found that at such small wavelengths conventional microwave technologies were no longer adequate. Instead we succeeded by utilizing far-infrared (FIR) technology based upon the principles of Gaussian optics. We find that these techniques greatly simplify the design and performance of the high-frequency ESR spectrometer, and they would be the natural way to proceed with submillimeter ESR spectroscopy in the future.

After describing our new design, we present initial experiments which illustrate the potential utility of FIR–ESR, particularly with respect to studies of motional dynamics. We then discuss possible future improvements and refinements for our 1-mm ESR spectrometer.

I. THE 1-MM SPECTROMETER

A. Description

Our 1-mm ESR spectrometer operates at 249.9 GHz and 8.9 T for $g = 2$. A schematic diagram of the instrument is shown in Fig. 1. The superconducting magnet was built by American Magnetics, Inc. (AMC) and has a maximum field value of 9.2 T at 4.2 K. In addition to the main 9.2-T coil, the field can be swept $\pm$ 500 G using an auxiliary superconducting field-sweep coil, which was constructed to minimize coupling to the main coil. Thus it can be swept while the main coil is persistent, making the spectrometer similar in field operation to a conventional ESR spectrometer operating at much lower frequencies. The maximum sweep rate we can achieve is about 35 G/s and it does not interfere with the main coil. The length of the magnet is 13.2 in., the outer diameter is 7.5 in., and the bore diameter is 2.4 in. The field homogeneity within a central 1-cm-diam spherical volume is better than $\pm 3\times10^{-6}$ without shims. Field persistence at 9 T is at least $1{:}1\times10^{7}$/h. The sweep coil was calibrated using the known hyperfine splitting of PDT in decane.[3b] The main coil is charged by an HP 6260B dc power supply which is controlled by an AMI 402A programmer. An HP 6032A dc power supply, with GPIB interface to a PC, ramps the sweep coil providing accurate and reproducible sweep rates. The leads supplying current to both main and sweep coils are nonretractable.

The Dewar is a warm bore design built by Cryofab, Inc. to accommodate our AMI magnet. The bore inner diameter is 1.75 in. and the outer diameter is 2.25 in. The diameter of the liquid-helium (LHe) chamber is 8.5 in., and its length is 48 in. A series of copper baffles and a liquid-nitrogen (LN_2) jacket, providing a 77-K shield in the warm bore, reduces the boil-off rate of the empty Dewar to about 0.4 ℓ/h. Boil off caused by the main and sweep coil current leads is minimized by using brass ribbons (0.004 in. thick, 0.25 in. wide, and 18 in. long) instead of copper as the current-carrying conductors in vapor-cooled leads similar in design to those used by Efferson.[4] Forty ribbons are used for each main lead (100 A) and 24 ribbons are used for each sweep lead (50 A). With the magnet and leads in place, the maximum LHe boil-off rate is less than 0.75 ℓ/h. Since our Dewar holds 12 ℓ of liquid above the magnet, the time available for experiments between LHe transfers is about 15 h. All helium gas blow off is collected for reliquefaction. An AMI liquid-helium level detector monitors the liquid level above the magnet. A liquid-helium transfer line extension inside the Dewar allows us to efficiently transfer liquid to the bottom of the Dewar,

 0034-6748/88/081345-07$01.30

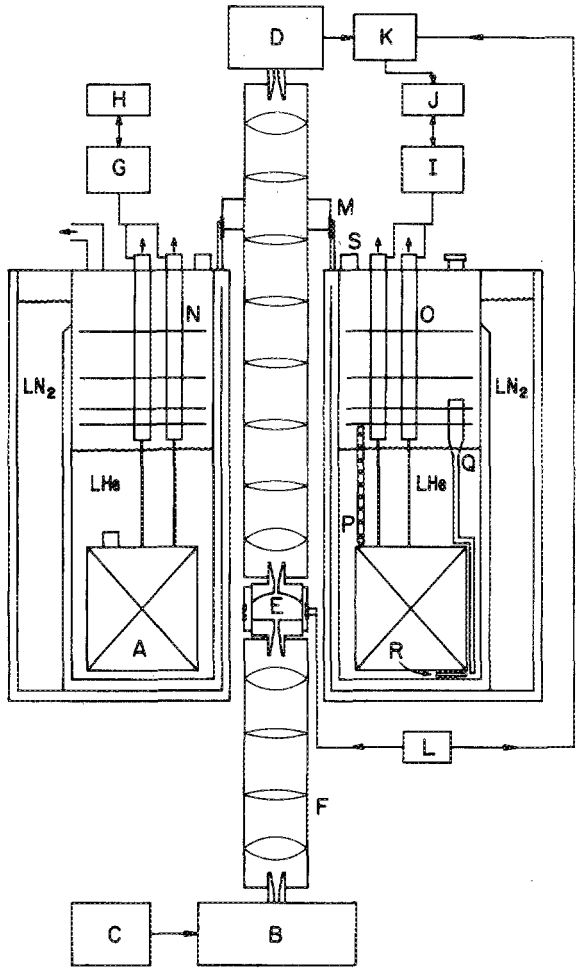

FIG. 1. Block diagram of 1-mm ESR spectrometer. A: 9-T superconducting solenoid and 500-G sweep coils; B: phase-locked 250-GHz source; C: 100-MHz reference oscillator for 250-GHz source; D: Schottky diode detector; E: Fabry–Perot semiconfocal cavity and field modulation coils; F: 250-GHz quasi-optical waveguide (Optiguide™); G: power supply for main coil (100 A); H: current ramp control for main magnet; I: power supply for sweep coil (50 A); J: PC which controls field sweep, data acquisition, and data manipulation; K: lock-in-amplifier for final signal amplification and detection; L: field modulation and lock-in reference source; M: Fabry–Perot cavity tuning screw; N: vapor-cooled leads for main solenoid (nonretractable); O: vapor-cooled leads for sweep coil (nonretractable); P: ^{4}He bath level indicator; Q: ^{4}He transfer tube; R: bath temperature/bath heater resistance pod; S: ^{4}He blow-off valves.

where a carbon resistor monitors the temperature during initial cool downs.

Our 1-mm source is a Millitech Corp. PLS-3F phase-locked source which delivers 5 mW at 249.9 GHz (WR-4 waveguide). See Fig. 2 for a diagram of the loop. The heart of the source is a Millitech GDM-10T Gunn oscillator phase locked to a highly stable 100-MHz reference (Program Test Sources model PTS 160). The Gunn output (40 mW) is locked to 83.3 GHz and then tripled to 249.9 GHz using a Millitech MU3-04T tripler. The source output can be swept within a $\pm$ 65-MHz range by sweeping the reference $\pm$ 25 kHz. The incident power may be attenuated as needed by inserting calibrated FIR attenuators (made from, e.g., carbon black) into the FIR beam.

Low-loss quasi-optical techniques[5] are used to propagate the millimeter wave beam from the source into the warm bore of the Dewar to the cavity and then on to the detector. Feedhorns are used to "launch" the linearly polarized beam from a waveguide mode to a free-space, TEM mode where the beam has a Gaussian amplitude distribution transverse to the direction of propagation. A Gaussian beam represents an adequate approximate solution to the wave equation, and can be propagated through free-space via a series of lenses. In our system (cf. Fig. 1) a Millitech scalar feedhorn propagates the HE_{11} mode and radiates close to a fundamental Gaussian wave into the TEM_{00} mode as it exits the source. The base of this horn contains a rectangular to circular waveguide transition, thus coupling the source waveguide to the horn itself. The diverging wave is focused by a focusing lens (diameter 0.89 in., focal length 1.08 in., beam waist radius 0.063 in.). Subsequently a series of longer focal length primary lenses (diameter 1.38 in., focal length 4.5 in., beam waist radius 0.26 in.) are used to propagate the beam over longer distances. Both focusing and primary lenses are made of Teflon and have antireflection surface grooves designed to minimize reflections at 249.9 GHz.

We have found the use of quasi-optical techniques at 1.2 mm much more efficient than that of waveguides. The loss incurred by the lenses over a 54-in. path length is only 2 dB, whereas the theoretical loss of WR-4 waveguide over the same distance is 16 dB. However, the large diameter of the lenses obstructs much of the air flow through the warm bore leading to frost buildup, unless the bore is enclosed in a dry nitrogen atmosphere.

Radiation is coupled into and out of the cavity by using two conical feedhorn/focusing lens pairs. The feedhorns were designed to couple to the beam waist radius w_0 of the focusing lenses, by the following simple relationship[5]:

$$w_0 = D/3, \tag{1}$$

where D is the aperture diameter of the horn. (This relation is true for low aperture phase error scalar horns.) In front of the detector, another conical feedhorn (from Custom Microwave)/focusing lens pair couples radiation from the TEM_{00} mode of the beam waveguide to the TE_{10} mode in WR-4 waveguide.

The cavity (Fig. 3) is a semiconfocal Fabry–Perot having 1-in. diam mirrors. The radius of curvature of the spherical mirror is 1 in.; the optimum intermirror distance for propagating the fundamental mode is approximately one-half the radius of curvature, or 0.5 in. This corresponds to a mode number, $\nu = 20$ (i.e., the number of half-wavelengths between the mirrors). The cavity is coupled to two homemade feedhorns by 0.060-in. (1.5-mm) diam coupling holes located at the center of each mirror. Because of the relatively large diameter of these holes, compared to the radiation wavelength, the loaded Q_L is only about 100, but this is quite satisfactory for the samples we have examined so far. (The Q is easily measured by first tuning the cavity between successive resonance to determine the finesse, $f = \lambda\Delta\lambda$, where λ is the tuning length between them and $\Delta\lambda$ is the full width of a single resonance. Then $Q_L = f\nu$.) In addition, the low Q has made tuning of the cavity very simple in our initial experiments. To tune the cavity, the spherical mirror is raised and

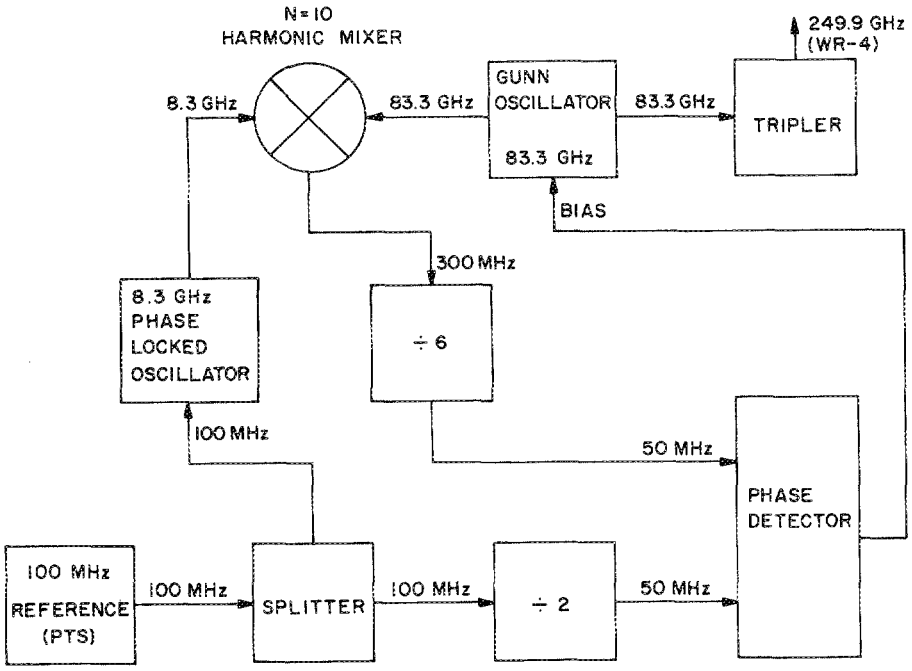

FIG. 2. Block diagram of 249.9-GHz source.

lowered with respect to the flat mirror by turning a homemade millimeter screw located at the top of the Dewar. One turn of the screw is approximately 0.5-mm vertical travel. The spherical mirror slides within a Teflon sleeve which is affixed to the lower, flat mirror. The flat mirror is fixed in a position such that samples placed on it are located within the region of maximum field homogeneity. The field modulation coil is wound around the Teflon sleeve (1.25 in. diameter, 0.5 in. length, 120 turns of No. 30 magnet wire) and embedded in GE varnish No. 1201 to eliminate noise at high modulation amplitudes.

Before each experiment, the cavity is tuned to resonance by rotating the millimeter screw until maximum transmission of radiation is found. For our detector (vide infra) it is necessary, during the tune-up, to amplitude modulate the radiation using a homemade (nonmagnetic) laser beam chopper, which we operate at 100 Hz. Once the cavity is tuned, the chopper is removed and the ESR signal is detected at the field modulation frequency.

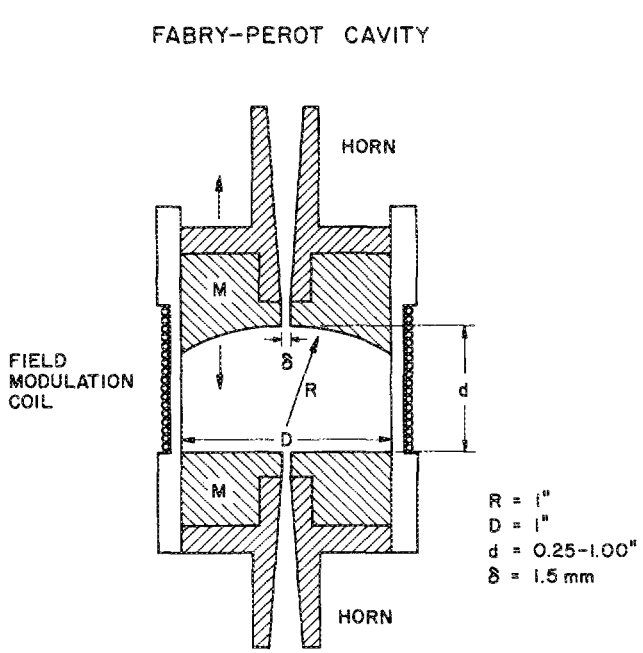

FIG. 3. Fabry–Perot cavity for 250 GHz. M indicates mirror assembly.

The detector is a Schottky diode (Millitech DXW-4F) having a tangential sensitivity of -46 dBm at 1 kHz. The diode is coupled to a low-noise video amplifier which is the noise-limiting component. It has a flat noise voltage N_v of < 10 nV/Hz over a 100-Hz to 30-kHz bandwidth, (i.e., $1/f$ noise has been suppressed). The diode detector has a flat responsivity R_0 of 3 V/mW over the bandwidth 100 Hz to 100 kHz. The noise equivalent power (NEP) of the detector–preamplifier system is given by $N_v/R_0 < 3\times 10^{-12}$ W/Hz. We have typically operated with a field modulation frequency of 0.5–1 kHz in view of the flat NEP due to absence of $1/f$ noise. The response of the detector is amplified by a PAR HR-8 lock-in amplifier and is then digitized and stored in a PC.

Sample holders (Fig. 4) for liquids were designed so as to minimize the amount of absorption of radiation by the holder material and to maximize the amount of liquid within the cavity. Holders were made from TPX (polymethylpentene) or Teflon, both of which exhibit low attenuation of millimeter waves. Liquids, which may first be degassed to prevent oxygen broadening, were placed within the holder and then "sealed" with a 5×10^{-4}-in.-thick Mylar film, stretched over the top of the sample holder by an O-ring. If the warm bore is swept continuously with nitrogen gas, the dissolution oxygen into the sample during the experiment can be prevented.

B. Ease of operation

The 1-mm spectrometer is fairly easy to operate. In fact, its operation is in a number of ways very similar to a conven-

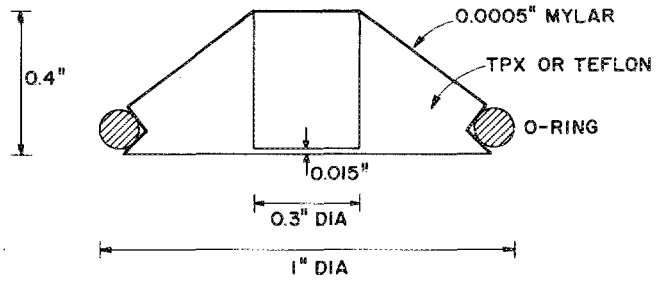

FIG. 4. 1-mm ESR sample holder for low loss samples.

tional 9-GHz ESR spectrometer once the main 9.2-T coil is ramped up to a field value near resonance. Then resonance is found by sweeping the sweep coil. The maximum sweep rate of 35 G/s is quite adequate when compared to a 9-GHz ESR spectrometer, and this is useful for the initial location of the resonance signal.

The solid-state source is very easy to operate since it is self-locking. It is much smaller than a FIR laser system (which can also operate at 1.22 mm), and it does not have the problems of stability and maintenance inherent with a laser.[6] Since our source delivers only 5 mW of power at 1 mm, alignment of lenses between source, cavity, and detector, and the alignment of the two cavity mirrors, is crucial to a successful experiment. There are two sets of lenses in our spectrometer (cf. Fig. 1). The lower set of lenses, between the source and the bottom cavity mirror, comprise one "Optiguide™" tube, and the top set of lenses, between the upper cavity mirror and the detector, comprise the other. To get an acceptable ESR S/N, the two Optiguide™ tubes, and therefore the two mirrors, must be properly aligned. This is currently done by manually adjusting the position of the bottom set of lenses. There is more than enough power, regardless of Optiguide™ and mirror alignment, to easily tune the cavity itself into resonance before each ESR experiment.

The length of time between liquid-helium transfers is 15 h, which is more than enough time to perform most experiments. If needed, it is possible to refill with liquid helium during an experiment. However, the subsequent change in warm bore temperature will cause the cavity length to change and cavity resonance to be lost. Better temperature control of the cavity should prevent this from happening in the future.

C. Performance characteristics

Resetability of the spectral line position has been investigated and deviations of no more than 2 G are observed. Usually the resettability is within 1 G, or one part in 10^5, of the applied field. There are no systematic deviations noted with respect to direction of field sweep or sweep rate. (Sweep rates of 0.3 G/s or less were used.) These deviations appear to be caused solely by the sweep coil and/or its residual coupling to the main coil.

From the experimental high-field spectra we have obtained (cf. Sec. II) we estimate a minimum number of observable spins as low as 10^{12} spins/G linewidths with no source attenuation (i.e., 5-mW incident power), a 500-Hz field modulation frequency, and a time constant of the lock-in detector of 10 s. For our resonator and sample holder, this would correspond to a minimum detectable molarity, $M_{\min}$ of 3×10^{-8} mol/G. This compares reasonably with an ESR spectrometer operating at 9 GHz.

II. ESR SPECTRA AT 250 GHZ

A. Polycrystalline samples

We show in Fig. 5 a derivative spectrum of polycrystalline pure DPPH both at 9 and 250 GHz. The spectrum at 9 GHz is the well-known exchange-narrowed result with a derivative linewidth of 2.4 G, but the one at 250 GHz covers over 70 G with considerable structure. In most studies of DPPH the g tensor is taken as isotropic, because its asymmetry is so small.[7–9] Only at higher frequencies (24–36 GHz) was it possible to just barely distinguish the anisotropy: $g_{\parallel}=2.0028$ and $g_{\perp}=2.0039$ (Ref. 10) for polycrystalline DPPH. The prominent outer splittings of the 250-GHz spectrum are 47.8 G apart in good agreement with assigning them to the parallel and perpendicular edges of the spectrum. This demonstrates how small anisotropies in g tensors virtually unobservable at 9 GHz are dramatically manifested at 250 GHz.

The source of the extra structure between the outer lines is not yet known. Based upon single-crystal x-ray studies and ESR studies at 9 GHz, there is more than one (typically 2 or 4) molecule per unit cell with different orientations.[7] Also, there are typically residual solvent molecules trapped in the crystal which can influence the crystal growth as well as the

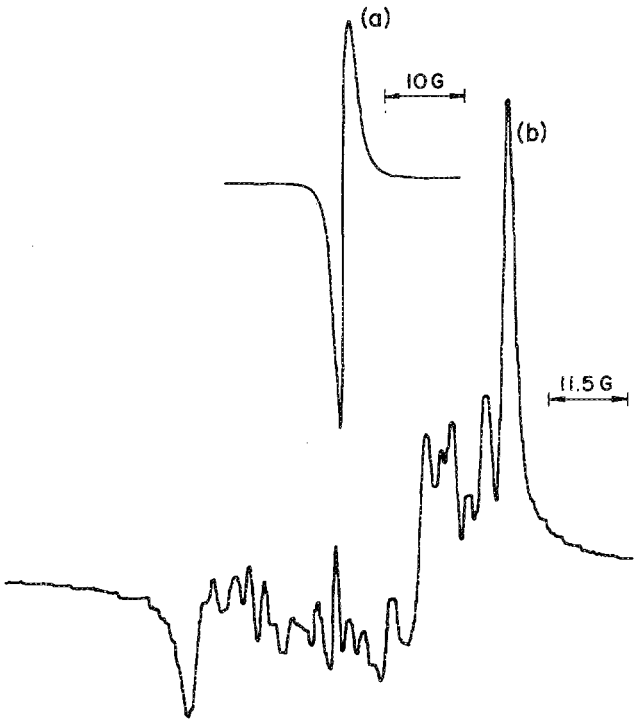

FIG. 5. ESR spectra of polycrystalline DPPH. (a) At 9.5 GHz; (b) at 250 GHz at room temperature.

structure of the unit cell. However, one would expect that any g-value differences between adjacent molecules would be averaged out by exchange as is the hyperfine tensor. That is, the exchange interaction has been estimated to be about $0.4\text{–}1\times10^{11}$ s^{-1} compared to $|g_{\parallel}-g_{\perp}|\beta_e B/\hbar\approx10^{9}$ for $B=9$ T (Ref. 11). Possibly the exchange is itself highly anisotropic, or else there is some heterogeneity in the properties of the individual microcrystals. Our main point is the greatly increased spectral sensitivity to such details at 250 GHz. Thus, future studies at 250 GHz (with single crystals) should be rewarding.

A sample of polycrystalline PD-Tempone also shows a single exchange-narrowed line at 9 GHz but at 250 GHz there is a broad spectrum corresponding to its asymmetric g tensor $g_x=2.0095$, $g_y=2.0063$, $g_z=2.0022$ (Ref. 12). There is some extra structure, but it is not as pronounced as for DPPH. (If the PD-Tempone is prepared in a highly concentrated smear with $CHCl_3$, then even at 250 GHz only a single exchange-narrowed line is observed, as it should be for strong exchange between randomly oriented molecules.)

B. Magnetically diluted liquid samples

We show in Fig. 6 the spectra obtained both at 250 GHz from 5×10^{-4} mol deoxygenated liquid-phase solutions of PD-Tempone dissolved in a series of mixtures of decane and mineral oil at $-6°$ to -10 °C. One immediately notices that the spectra at 250 GHz are much broader than those at 9 GHz. Most of these spectra are in the motionally narrowed regime, so that they consist of three Lorentzians from the ^{14}N isotropic hyperfine interaction. The very sharp line spectra obtained at 9 GHz show very little change with increasing viscosity. In fact, only by studying the small differences in linewidth amongst the hf (hyperfine) lines is it possible to determine the rate of the rotational tumbling that is averaging out the hyperfine and the g tensor.[3,13] The linewidths at 250 GHz are more dramatically affected by increasing the viscosity. This is illustrated in Fig. 7 where the linewidth of the central line is plotted as a function of viscosity for both frequencies. One notes an initial moderate decrease followed by an increase in linewidth with viscosity at 9 GHz, but a substantial systematic increase with viscosity at 250 GHz. This is consistent with theory,[13] which predicts a quadratic dependence on field (or frequency) of the g-tensor contribution to this linewidth, so that at 250 GHz it predominates over other sources of line broadening. (Its contribution is linear in the viscosity for a single solvent.) As a result, the 250-GHz linewidths are very useful in estimating rotational relaxation in the motionally narrowed regime. Note that τ_R, the rotational correlation time varies over more than an order of magnitude (6.5 ps for pure decane to about 150 ps in mineral oil).

At 9-GHz spin-rotational relaxation and spin exchange make significant contributions, and their contributions to the width have inverse dependence on visocity.[3,13] When combined with the g-tensor contribution, the viscosity dependence is nonlinear at 9 GHz and more difficult to interpret. Futhermore, there are fundamental questions about the frequency dependence of the spin relaxation[3,13] which could be addressed by combining studies at 9 and 250 GHz.

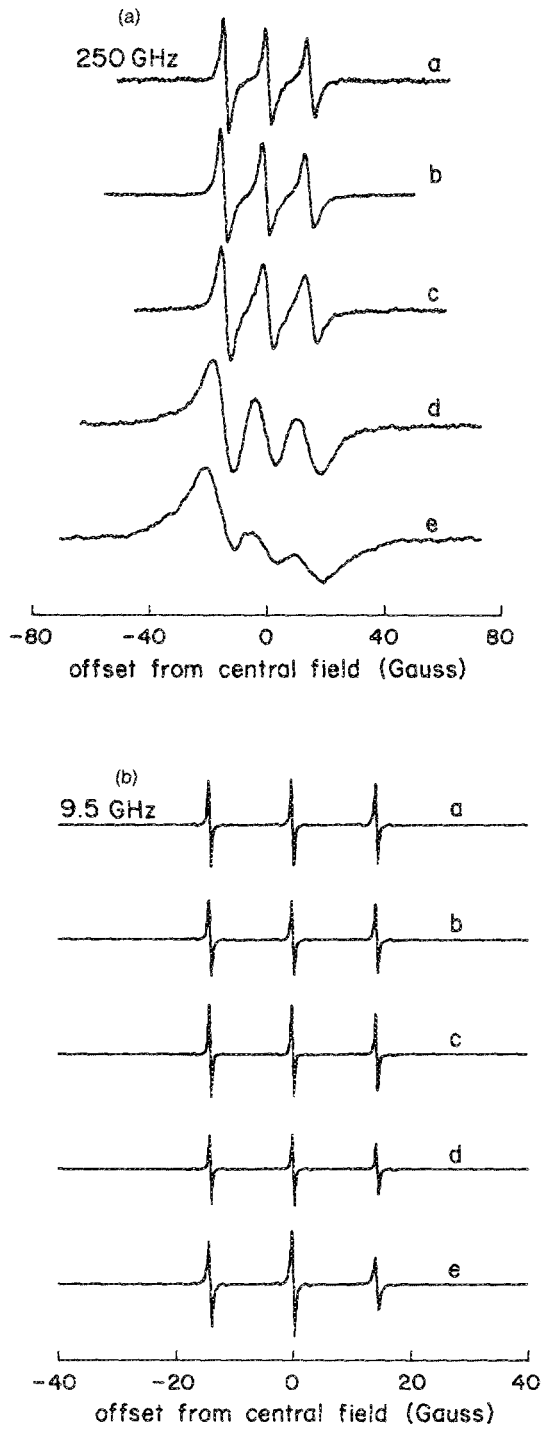

FIG. 6. ESR spectra of the stable nitroxide radical: PD-Tempone (5×10^{-4}) in solvent mixtures of n-decane and mineral oil at temperatures of $-6°$ to -10 °C. (a) 250-GHz spectra, (b) 9-GHz spectra: a: 100% decane; b: 73.7% decane; c: 50.9% decane; d: 19.2% decane; 3: 100% mineral oil. All samples are deoxygenated except for (a) e. The sequence of solvent mixtures a through e exhibits increasing viscosities.

In the case of pure mineral oil solvent at 250 GHz the ESR spectrum is no longer in the motionally narrowed regime, and simple relaxation theory no longer applies. This is evidenced by the large overlap of the hf lines as well as the fact that the width is significantly less than anticipated from the 9-GHz results. This slow-motional regime sets in for val-

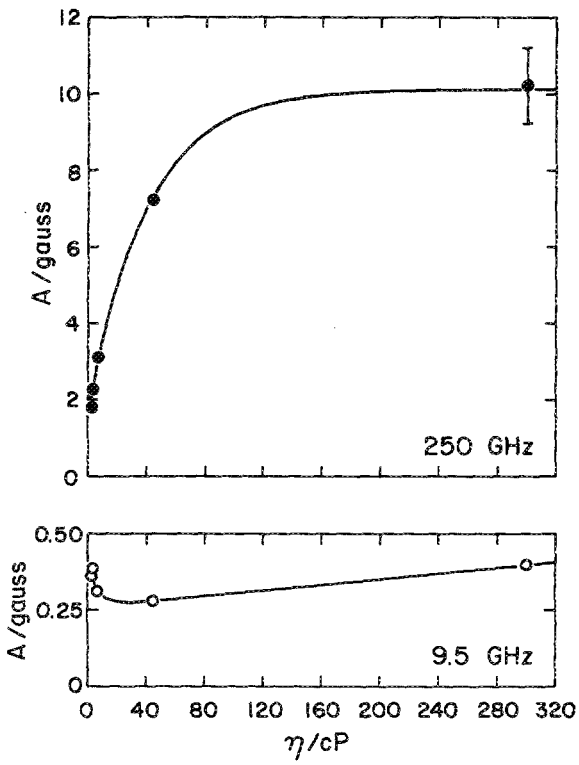

FIG. 7. T_2^{-1} in Gauss for central hf line of spectra shown in Fig. 6 for 250 and 9.5 GHz plotted as a function of solvent viscosity. (The viscosities of the solvent mixtures were measured by standard methods.) The datum with the large error bar is from spectrum (a) e of Fig. 6, for which a deoxygenated width was estimated by extrapolation.

ues of $\tau_R \gtrsim 10^{-10}$ s (100 ps) for nitroxides at 250 GHz. This is about one order of magnitude faster than for 9 GHz (Ref. 12). It is well known that slow-motional spectra afford the opportunity to obtain more detailed information on the dynamics than fast-motional spectra.[12] This is another important application for such high-frequency ESR studies.

III. IMPROVEMENTS TO THE SPECTROMETER

There are several improvements to the spectrometer that can be made in order to enhance its sensitivity. First, one could increase the loaded Q, or Q_L of the Fabry–Perot resonator. Values of 10^4–10^5 are, in principle, possible with loss-free samples. For the resonator of Fig. 3, the dominant contribution to Q_L comes from the large cavity coupling holes. A convenient rule of thumb[14] for making coupling holes to resonators in this frequency band is

$$a \approx \lambda/3, \tag{2}$$

where a is the diameter of the coupling hole and λ is the wavelength of radiation. For $\lambda = 1.2$ mm we find from Eq. (2) $a \approx 0.4$ mm, whereas $a = 1.5$ mm for the resonator in Fig. 3. This results in a substantially overcoupled resonator. In fact, the beam waist at the flat mirror may be calculated[15] to be $w_0 = 2.2$ mm. Thus, in our present resonator, most of the radiation illuminates the coupling holes, not the mirrors.

In future experiments, we plan to use a resonator with smaller coupling holes chosen according to Eq. (2). This is not expected to be an unmitigated advantage. High-Q cavities require more critical frequency tuning. Currently, we are able to align the top and bottom Optiguide™ tubes (and hence the two cavity mirrors) by turning a millimeter screw at the top of the Dewar and adjust, by hand, the position of the lower tube assembly. This arrangement would have to be replaced by translation stages to lower and raise the tubes and to move them horizontally in the x–y plane. However, this would improve cavity tuning and alignment for maximum S/N. It would also allow us to move the sample precisely into the region of highest field homogeneity. The stages could also be used in a feedback loop to keep the cavity tuned to resonance during an experiment. This would almost certainly be necessary for resonators having a very high Q, where small temperature fluctuations and vibrations could easily lead to significant fluctuations from resonance.

Another problem with a high-Q resonator would be the need to retune the coupling holes as samples are changed. The unloaded Q or Q_u of such a resonator would largely be determined by sample losses requiring readjustment to provide optimum coupling of the FIR radiation. We do not, at present, have a convenient design for accomplishing this, and it is, in fact, not needed for the substantially overcoupled resonator of Fig. 3.

Let us now examine an expression for the minimum detectable number of spins for a transmission spectrometer[16,17]:

$$N_{\min} \propto (\eta Q_u \omega_0)^{-1}[(Q_u + Q_r)/Q_L] \times (\Delta H_{pp}/H_0)(\Delta H_{pp}/H_{mod})(3kT_d \Delta f)^{1/2} \times [F_k - 1 + (t + F_{amp} - 1)L]^{1/2} P_w^{-1/2}, \tag{3}$$

where Q_r is the radiation Q, F_k is the noise figure of all components before the detector, T_d is the detection temperature, t is the dimensionless noise temperature of the detector (in units of T_d), L is the insertion loss of the detector, F_{amp} is the noise figure of the audio preamplifier with Δf the effective bandwidth of the audio lock-in detector and output time constant. Also, P_w is the mm wave power, ω_0 and H_0 are the mm wave frequency and the dc field strengths, ΔH_{pp} is the derivative peak-to-peak linewidth, and H_{mod} is the amplitude of the modulating field. It has been assumed that $H_{mod} \ll H_{pp}$ and that the signal is not saturated. Also the frequency scaling in Eq. (3) is really applicable for equivalent designed resonators.[16] From Eq. (3) we see that for a matched resonator with $Q_r = Q_u \approx 10^4$ a factor of 100 improvement in sensitivity is to be expected over our present case of $Q_L \approx Q_r \approx 100$. (More generally, of course, $Q_L^{-1} = Q_u^{-1} + Q_r^{-1}$.)

We can also anticipate improved S/N by utilizing higher-frequency field modulation, (e.g., 100 kHz) in place of 1 kHz. The lower-frequency field modulation is more convenient, and higher frequencies are not required by the flat frequency sensitivity of the detector in the frequency band of interest (it is limited by generation-recombination noise). However, the noise figure of the frequency-locked source, which contributes to F_k and the noise figure of the amplifier F_{amp} which affect the sensitivity [cf. Eq. (3)], can be modeled approximately by a $1/f$ dependence. Thus, their perfor-

mance should be significantly improved at higher field modulation frequencies as would effects of microphonics. The use of higher-frequency field modulation would be facilitated by constructing the resonator with a minimum amount of bulk metal to circumvent skin-depth effects.

One could also improve the sensitivity by working at higher millimeter wave power [cf. Eq. (3)], at least until saturation of the transition sets in. We have never observed any indication of spectral saturation at 5 mW of incident power. The Thomson CO-12 "carcinotron" with 500-mW maximum power in the band 226–274 GHz may provide a means to increase P_w; we note, however, that carcinotrons are noisier than solid-state sources, even with frequency and phase locking,[18] thus contributing to F_k and partially offsetting the advantage of a larger P_w.

Simple theoretical estimates of sensitivity based upon Eq. (3) do suggest that the NEP of the detector/preamplifier system is a principal limitation to our sensitivity. It should be possible to improve on the noise figure by the use of a low-temperature bolometer detector/preamplifier system.[19,20]

Another important improvement would be temperature variation and control. For *cooling*, we are at present limited to flowing precooled N_2 through the narrow (0.135-in.) annular radius between the warm bore and the Optiguide™. This does not provide adequate temperature variation and control. This problem may be solved by using a set of smaller diameter lenses between the source and the resonator, thereby increasing the free-annular radius.

The beam waist of the lenses in an Optiguide™ tube must be an appropriate, small fraction of the lens diameter to ensure that the Gaussian beam is not distorted by aperture limitations.[21] Since the beam waist is simply related to the focal length for fixed wavelength in a confocal system,[5] one can show

$$N_t/N_2 = (D_1/D_2)^{-2} \tag{4}$$

per unit length of Optiguide™ run. D is the diameter of the lenses in the Optiguide™ system containing N lenses. In this frequency band,[21] the insertion loss per lens is approximately 0.1–0.2 dB. Thus, one cannot go to arbitrarily small Optiguide™ diameter in order to maximize the annular radius, because the insertion loss becomes unacceptably large. Another way of stating this is that increasing the number of lenses contributes to F_k in Eq. (3).

As a reasonable compromise, it should be possible to replace the present lower Optiguide™ system (lens diameter of 1.38 in.) with an Optiguide™ system having a 1-in. outer diameter. This will approximately double the contribution to F_k from the Optiguide™ below the resonator and above the source. It is not a major noise term in F_k, however, so we expect that F_k will change only slightly.

With the increased annular radius, ($\frac{3}{8}$ in.) it will also be possible to flow precooled (or heated) fluid or gas directly to a temperature jacket in good thermal contact with the mirrors of the Fabry–Perot resonator.

On the other hand, heating can readily be achieved with resistors placed in thermal contact with the lower mirror assembly upon which the sample rests. By this means we are able to vary the temperature from about − 20 °C (ambient) to about + 100 °C.

Finally, we mention that the sample holder shown in Fig. 4 is appropriate for low loss liquids, since the height of fluid is typically several wavelengths. It has proven very successful for hydrocarbons (cf. Sec. II) and other low loss solvents such as thermotropic liquid crystals (e.g., Merck Phase V). Lossy solvents, such as water, would require a different sample holder that maintains the height of the fluid no more than about 0.1 mm above the lower mirror when inserted into the Fabry–Perot resonator, since this is a region of low E field.[22]

ACKNOWLEDGMENTS

We wish to thank Dave Schneider, Dan Igner, and Dave Bazell for their help during the early stages of spectrometer design and David Budil for his help with the manuscript. We thank Eric Smith and David M. Lee for their advice on the design of the magnet Dewar.

This work was supported by NIH Grant No. GM25862 and NSF Grants Nos. CHE8703014 and DMR-8616727.

[a] Present address: Advanced Materials Corp., Mellon Institute, 4400 Fifth Avenue, Pittsburgh, Pennsylvania 15213.

[1] O. Ya. Grinberg, A. A. Dubinski, and Ya. S. Lebedev, Russ. Chem. Rev. **52**, 850 (1983).
[2] E. Haindl, K. Möbius, and H. Oloff, Z. Naturforsch. **40a**, 169 (1985).
[3a] A preliminary account of this work was presented at the 10th International EPR Symposium, Rocky Mt. Conference, Denver, CO (Abstracts, August 1987); [3b] S. A. Zager and J. H. Freed, J. Chem. Phys. **77**, 3344 (1982).
[4] K. R. Efferson, Rev. Sci. Instrum. **38**, 1776 (1967).
[5] P. F. Goldsmith, in *Infrared and Millimeter Waves*, edited by K. Button (Academic, New York, 1982), Vol. 6, p. 277.
[6] For example, W. A. Peebles, N. C. Luhmann, Jr., A. Mase, H. Park, and A. Semet, Rev. Sci. Instrum. **52**, 360 (1981).
[7] R. W. Holmberg, R. Livingston, and W. T. Smith, Jr., J. Chem. Phys. **33**, 541 (1960); Y. K. Kim and J. S. Chalmers, *ibid.* **44**, 3591 (1966).
[8] N. W. Lord and S. M. Blinder, J. Chem. Phys. **34**, 1693 (1961).
[9] J. S. Hyde, R. C. Sneed, Jr., and G. H. Rist, J. Chem. Phys. **51**, 1404 (1969).
[10] P. P. Yodzis and W. S. Koski, J. Chem. Phys. **38**, 2313 (1963); B. M. Kozyrev, Yu V. Yablokov, R. O. Matevosjan, M. A. Ikrina, A. V. Iljasov, Yu. M. Ryshmanov, L. I. Stashkov, and L. F. Shatrukov, Opt. Spectra **15**, 340 (1963).
[11] G. Pake and T. Tuttle, Phys. Rev. Lett. **3**, 423 (1959).
[12] J. H. Freed, in *Spin Labeling: Theory and Applications*, edited by L. J. Berliner (Academic, New York, 1976), Chap. 3.
[13] S. A. Goldman, G. V. Bruno, C. F. Polnaszek, and J. H. Freed, J. Chem. Phys. **56**, 716 (1972); *ibid.* **59**, 3071 (1973); J. S. Hwang, R. P. Mason, L. P. Hwang, and J. H. Freed, J. Phys. Chem. **79**, 489 (1975).
[14] P. Goy, in *Infrared and Millimeter Waves*, edited by K. Button (Academic, New York, 1983), Vol. 8, p. 352.
[15] G. W. Chantry, *Long Wave Optics*, Vol. 1 (Academic, New York, 1984), p. 68.
[16] C. F. Poole, *Electron Spin Resonance* (Interscience, New York, 1967), p. 546.
[17] G. Feher, Bell Syst. Tech. J. **36**, 449 (1957); G. K. Fraenkel, in *Technique of Organic Chemistry: Physical Methods*, Vol. I, Part IV, edited by A. Weisberger (Interscience, New York, 1960).
[18] A. van Ardenne, E. E. M. Woestenburg, and L. J. van der Ree, Rev. Sci. Instrum. **57**, 2547 (1986).
[19] J. W. Archer and M. T. Faber, Microwave J. **27**, 135 (1984).
[20] A. T. Wijeratne, G. L. Dunifer, J. T. Chen, and L. E. Wenger, Phys. Rev. B **37**, 615 (1988).
[21] Ellen Moore (private communication).
[22] Note that the dielectric loss term ϵ'' for water is only 5.25 at 250 GHz compared to 32.6 at 9.35 GHz; P. R. Mason, J. B. Hasted, and L. Moore, Adv. Mol. Relaxation Processes **6**, 217 (1974); A. M. Bottreau, J. M. Moreau, J. M. Laurent, and C. Marzat, J. Chem. Phys. **62**, 360 (1975).